Copula-based Method to Generate Consistent Surface Pressures Under Uncertainty

Aaron C. Burkhead* and Derek J. Dalle†
NASA Ames Research Center, Moffett Field, CA 94035

This paper establishes a method to create surface pressure databases that allow for uncertainty quantification. Aerodynamic databases are critical products for launch vehicles and other aeronautical systems, and surface pressure databases are one such database that constains large quantities of data. The focus of this work is the relationship between the integrated force and moment database and the surface pressure database. In particular, the work attempts to provide a method that maintains consistency between these two databases when accounting for uncertainty. The integrated force and moment database and surface pressure databases are constructed from CFD data which is high-density but low-trust. However, the force and moment database will often also include data from high-trust but low-density sources such as from wind tunnel experiments. This means that the quantified uncertainty of the force and moment database is higher quality as it includes this high fidelity wind tunnel data. This motivates the idea to use the force and moment database uncertainty when constructing the surface pressure database uncertainty. The method utilizes the statistical idea of a copula in order to generate surface pressures that match with uncertain integrated force and moment distributions as well as being consistent with known CFD data. This statistical consistency is quantified by using the Maximum Mean Discrepancy two-sample test. The predictive error of the method is also approximated using leave-one-out error estimation and the good overall performance of the method is presented using probability boxes in a simulated uncertainty scenario.

I. Motivation

A crucial task during the analysis of an ascent vehicle is to estimate the integrated forces and moments on the vehicle at many points along the vehicle's potential trajectory by Computational Fluid Dynamics (CFD). Engineers can then collect these results and create a force and moment database, which can then be interpolated to predict the integrated forces and moments at any arbitrary flight condition. These force and moment databases can include an uncertainty model, e.g. in [1], so that each force and moment coefficient at a given flight condition is actually a probability distribution rather than a single deterministic value.

In addition to the integrated force and moment database, a database of surface pressures across the vehicle can also be provided. It is logical that querying the integrated force and moment database and the surface pressure at the same flight condition should return a result that is in agreement with each other. Essentially meaning that integrating the surface pressure should return the same force and moment values that the integrated force and moment database itself returns. However, factoring in the difference in data sources between the databases makes this more challenging. The integrated load database can, and should, be constructed using a mix of CFD data and higher fidelity wind tunnel data. Whereas the surface pressure data is exclusively taken from CFD simulations. The developing work of using pressure sensitive paint in wind tunnels may allow experimental surface pressure data to be used in future databases [2], but in this work only the integrated forces and moments are considered to have high-fidelity experimental data sources. Taking into account that the force and moment data should contain experimental data, and it is relatively simple to construct an uncertainty model for them as they are scalar values, the goal for this work is to provide an uncertain surface pressure distribution, based only on the CFD data, that is consistent with the quantified uncertainty in the integrated forces and moments.

There are existing works that have investigated methods to generate these kinds of surface pressures, such as the previous work in [3] that investigates an adjustment method for surface pressures on NASA's Space Launch System that allows for the construction of a surface pressure that integrates to match target force and moment values. The method provided in this work builds off these earlier efforts by using a copula-based approach in order to generate surface pressures that integrate to force and moment values sampled from their corresponding uncertain distributions. The key addition of this work that was not accounted for in the prior work is to generate uncertain surface pressures that have a

*Aerospace Eng., Computational Aerosciences Branch, Member AIAA, aaron.c.burkhead@nasa.gov
†Aerospace Eng., Computational Aerosciences Branch, Member AIAA, derek.j.dalle@nasa.gov

statistically insignificant difference with the known CFD surface pressures, essentially attempting to root the generated surface pressures to the known CFD data. The reason for this is to try and ensure that the generated surface pressures are not arbitrarily constructed and that they obey the spatial relationships between each of the surface pressure points in the known data. The validation of this is done by sampling known integrated force and moment data and generating new possible surface pressures that integrate to these sampled values. This sampling and generating is done many times and in the end the generated surface pressures are compared with the known data to determine if they are statistically similar. The Maximum Mean Discrepancy [4] 2-sample test is chosen to compare the distributions of the generated and known surface pressures. The significance level parameter α was set to 0.05 for the test, corresponding to a 95 percent confidence level. The critical score required by the test was determined by using the bootstrapping approach that is suggested by Gretton et al. [4].

The rest of the paper is outlined as follows. First, the set of data used in the work is shown and then the method for generating consistent surface pressures and is described. Next, the results of validating the method via the Maximum Mean Discrepancy test, the estimation of the leave-one-out error, and performance of the model in a simulated uncertainty scenario are presented. Finally, a brief discussion of potential future work and concluding remarks are included.

II. Dataset

The surface pressure data used in this work was taken from CFD simulation results on a generic ascent vehicle geometry. The launch vehicle geometry selected for study was a hammerhead rocket design [5] with several simple protuberances added. Figure 1 shows the vehicle geometry used in the generation of the dataset.

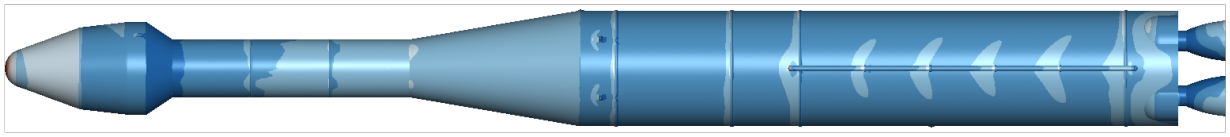


Figure 1. Hammerhead geometry used to generate the dataset.

This dataset varied the vehicle angle of attack (α) and angle of sideslip (β). The values (α,β) were set by fourth level nested Clenshaw-Curtis quadrature points [6] shown in Figure 2. The Mach numbers for all the CFD simulations used in this dataset were fixed at M=1.8.

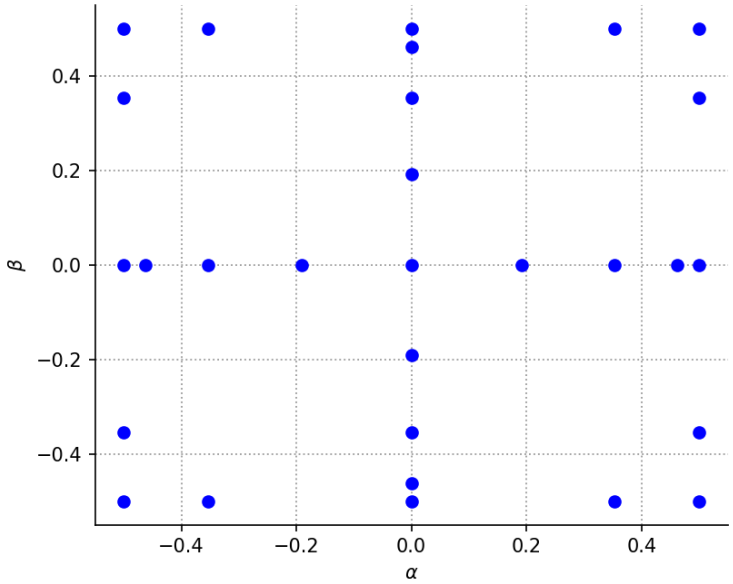


Figure 2. α & β values used in the flight orientation dataset.

The FUN3D 13.7 code [7] from NASA Langley Research Center was used to compute the CFD solutions. The simulations solved the compressible, calorically perfect gas governing flow equations using a steady local time step pseu-

dotime advancement scheme. They used the Spalart-Allmaras turbulence model and Harten-Lax-van Leer-Contact flux construction with the stencil-based van Albada flux limiter augmented with a heuristic pressure limiter. A triangular unstructured surface mesh was used with volume cells generated via AFLR3[a]. Once the CFD was run, the integrated forces and moments as well as the surface pressures were extracted from each case. The NASA CAPE[b] software was used in both executing the required CFD cases and the post-processing of the resulting data.

In order to simulate querying from a database, response surfaces were built using the distributed load data from the n_c=29 CFD solutions. These response surfaces were built using Gaussian Radial Basis functions with bandwidths equal to the average distance between the α and β locations shown in Figure 2. The response surfaces were sampled at N_s uniformly distributed points within the CFD bounds for α and β, i.e. points drawn from $\mathcal{U}(-0.5, 0.5)$ for both variables. The N_s=1000 sampled surface pressures were taken to be the full surface pressure dataset used in this work. The surface pressures extracted from each case are stored as a vector with n=402909 values, representing the data over the spatial locations of the vehicle geometry.

III. Method

Utilizing the notation and definitions contained in [**?**], each CFD simulation results in a surface pressure solution $\mathbf{c}_{p,i}$. These surface pressures can be integrated to provide aerodynamic force and moment coefficients on the vehicle. The notation used for the six integrated coefficients are C_A, C_N, C_Y, C_{LL}, C_{LM}, and C_{LN} for the axial force, normal force, side force, rolling moment, pitching moment, and yawing moment respectively.

Similarly to the work in [8] and [9], the dispersion method begins by essentially performing Principal Component Analysis on the CFD surface pressure data. First, the Singular Value Decomposition (SVD) is utilized in order to generate the basis vectors which are then used to construct new potential surface pressures. The n_c=29 surface pressure arrays are stacked into a snapshot matrix. For example, the snapshot matrix for the surface pressure profiles $\mathbf{c}_{p,i}$ would be $\mathbf{C}_p = [\mathbf{c}_{p,1}, \mathbf{c}_{p,2}, \ldots, \mathbf{c}_{p,n}]$. This matrix has the dimensions $n \times n_c$, with n being the number of nodes in each surface pressure and n_c being the number of surface pressure cases.

Before performing the SVD, the average over the n_c cases for surface pressure node is subtracted from $\mathbf{C}_p$. The resulting matrix, $\mathbf{C}'_p$, represents a surface pressure perturbation matrix, also referred to later as the delta surface pressure, and is the matrix on which the SVD is performed, as shown below.

$$\text{SVD}(\mathbf{C}'_p) = \mathbf{U}_p \mathbf{\Sigma}_p \mathbf{V}_N^T \tag{1}$$

The diagonal of $\mathbf{\Sigma}_p$ contains the singular values and $\mathbf{V}_N^T$ is a matrix containing the right singular vectors. These matrices are not directly used in this method. The columns of $\mathbf{U}_p$ contain the orthonormal bases that will be used to construct the surface pressure dispersion. The number of bases resulting from this depends on n_c; it will provide up to n_c orthonormal bases. In general, the number of bases kept for the next step will be labeled κ.

First, the κ selected basis vectors from $\mathbf{U}_p$ are used to build a linear estimation to each of the n_c surface pressures used in the snapshot perturbation matrix $\mathbf{C}'_p$. This is done by solving the linear system below for the coefficients ω_i, where the matrix $\tilde{\mathbf{U}}_p$ contains the κ bases vector columns kept from $\mathbf{U}_p$.

$$\tilde{\mathbf{U}}_p \omega_i = \mathbf{c}_{p,i} \tag{2}$$

The result is n_c arrays of κ coefficients, that can be stacked into a $\kappa \times n_c$ matrix, $\mathbf{\Omega}$. The next step is to generate surface pressure dispersions using coefficients that follow the joint distribution of the coefficients in $\mathbf{\Omega}$. The goal of this being to use these coefficients as a lower dimensional proxy for the full joint distribution of the known surface pressure data.

After the coefficients $\mathbf{\Omega}$ are found, the next step is to use them in order to generate new surface pressure that could come from the distribution implied by the known data while also integrating to given target forces and moments. The statistical concept of a copula [10] motivates a method to achieve this. A copula is effectively a decomposition of a multivariate statistical distribution into a multivariate distribution containing the dependence structure between the variables and univariate marginal distributions for each variable. Start with a random vector $(x_1, x_2, ..., x_d)$, with continuous marginal cumulative distribution functions (cdf) $F_i(x) = P(x_i < x)$. Applying the cdfs to the random vector results in

$$(u_1, u_2, ..., u_d) = (F_1(x_1), F_2(x_2), ..., F_d(x_d)), \tag{3}$$

with each u_i uniformly distributed on $[0, 1]$. The copula of the random vector $(x_1, x_2, ..., x_d)$ is then the joint cumulative distribution function $C(u_1, u_2, ..., u_d)$. In this use case, the copula is used in order to pseudo-randomly draw variables

[a]https://www.simcenter.msstate.edu/software/documentation/aflr3/index.html
[b]https://github.com/nasa/cape

from the distribution underlying the random vector. The process to draw a new random vector sample x^* simply takes a random sample from the copula $u^* = (u_1^*, u_2^*, ..., u_d^*)$ and applies the inverse marginal cdfs F_i^{-1} as

$$x^* = (F_1^{-1}(u_1^*), F_2^{-1}(u_2^*), ..., F_d^{-1}(u_d^*)). \tag{4}$$

Applying this sampling process to the coefficients $\mathbf{\Omega}$ to draw a new coefficient sample ω^* is done by first approximating the copula of $\mathbf{\Omega}$. This is done with a multivariate Gaussian distribution $\mathcal{N}(0, \sigma)$, with σ being the estimated covariance matrix of $\mathbf{\Omega}$. A sample is drawn from $\omega' \sim \mathcal{N}(0, \sigma)$, then the marginal cdfs of $\mathcal{N}(0, \sigma)$ are applied to ω' resulting in ω^u. This new sample is bound by the inverval $[0, 1]$ but maintains the dependence structure of $\mathcal{N}(0, \sigma)$, and thus approximately the dependence structure of $\mathbf{\Omega}$. Finally, the inverse marginal cdfs of $\mathbf{\Omega}$ are applied in each dimension to approximately recover a novel coefficient sample $\omega^* = (F_1^{-1}(\omega_1^u, F_2^{-1}(\omega_2^u, ..., F_d^{-1}(\omega_d^u))$. The integral of the surface pressure generated from the new coefficient sample can be any value. If the goal is to generate a surface pressure that integrates to target integrated values, then a small modification can be made the to sampling process. The inverse marginal cdfs that are applied can be conditioned on the target integrated values first $F_i^{-1}(\omega_i^u | C_A, C_N, ...)$. This results in surface pressures that are normally distributed about the target integrated values. Many samples can be drawn in this fashion and, for the results included in this work, the sample with the largest probability density is taken as the generated surface pressure. Another potential criteria could be to chose the surface pressure with the smallest errors to the target integrated coefficients. Regardless of the selection approach, due to the statistically generated nature of the surface pressure, it is likely that there will be a difference between the target integrated coefficients and the integrated values of the generated surface pressure. If an exact match of integrated coefficients is required, a small correction to the surface pressure can be applied using the adjustment mode ideas in [8]. If the error is small the correction to the coefficients should also be small enough to maintain statistical consistency.

The inverse conditioned marginal cdfs used are constructed using gaussian kernel density estimation to approximate the joint probability distribution $p(\omega_i, C_A, C_N, ..., C_{LN})$. While the conditioned probability distribution $p_{\mathbf{cond}}(\omega_i | C_A, C_N, ..., C_{LN})$ is numerically estimated by sampling p over the domain of values of ω_i with fixed values for the integrated coefficients C_A, C_N, etc. Using Gaussian kernel density estimation on this 7-dimensional datasx distribution is reaching the practical limits of the technique. Previous work suggests 6-dimensional data as the upper limit for an effective application of the technique [11], however recent work suggests it can perform poorly in as few as 4 dimensions [12]. It is possible to get around this dimensionality problem by conditioning the inverse marginal cdfs on a smaller subset of the integrated aerodynamic coefficients. This leaves the unconditioned variables to vary somewhat freely, which could be justified since the strong correlations to capture are only between C_N and C_{LM} and between C_Y and C_{LN}. The rotational moment C_{LL} is also quite small and not a large factor in the dataset used for this work so leaving it out of the conditioning step could be justified. However, the work presented here simply uses the 7-dimensional data as mentioned prior.

IV. Results

A. Validation

As mentioned in the introduction, the goal for the method described in this work is to generate surface pressures that follow the probability distribution of the surface pressures from the CFD data. The test used to compare is the Maximum Mean Discrepancy two-sample test. However, if the method is applied to an uncertain integrated force and moment at a single point the resulting surface pressures are not expected to match the overall distribution of the CFD data. It should be restricted to a limited space of the distributed load probability distribution corresponding to the uncertain integrated value bounds. Instead of attempting to test this limited space, the validation test used in this work is as follows. First, N_d values are drawn from the integrated forces and moments data, with equal probability and no replacements. Then, the method will generate a distributed load that integrates to each of these drawn values. The resulting collection of surface pressures are then tested, with the Maximum Mean Discrepancy two-sample test, against the known distributed loads to determine if the difference between the generated distribution and the known distribution is statistically significant. A significance level of 0.05 is chosen for this validation test. This level is the chosen upper bound on the probability of falsely rejecting that the two samples come from the same distribution [4]. If the method can generate surface pressures that pass this validation test then it is considered validated as a method that can generate surface pressures that follow the known distributed load distributions from CFD.

This validation test was performed with a simultaneous draw of $N_d = 100$ force and moment coefficients from known data cases. Figure 3 shows histogram comparisons of generated surface pressures (red) with the known data used in the conditional marginal distribution estimates (blue). The distributions of the generated data and the known data in these histograms look to be similar in a qualitative inspection. The histograms at $c_{p,200000}$ and $c_{p,300000}$ give a clear example of the qualitative success of the method to match well with the known data. These histograms are skewed

with easily apparent modes that the generated results are able to replicate. The generated surface pressures passed the MMD test as shown in Table 1. The surface pressure data only compared the distributions of ω, the method's linear construction coefficients, as the dimensionality of the actual surface pressure data makes the test computationally too expensive. This is justified as the method had been applied to smaller dimensional line load data previously and the MMD test results show that comparing the distributions of the coefficients always had the same concluding results as comparing the line load distributions directly. There is no guarantee the trend will hold for surface pressure data but it is not feasible to test the full dimensional data. This is due to statistical testing in this way being a challenge in just tens of dimensions, so testing the hundreds of thousands of dimensions of the surface pressure data is currently not realistic.

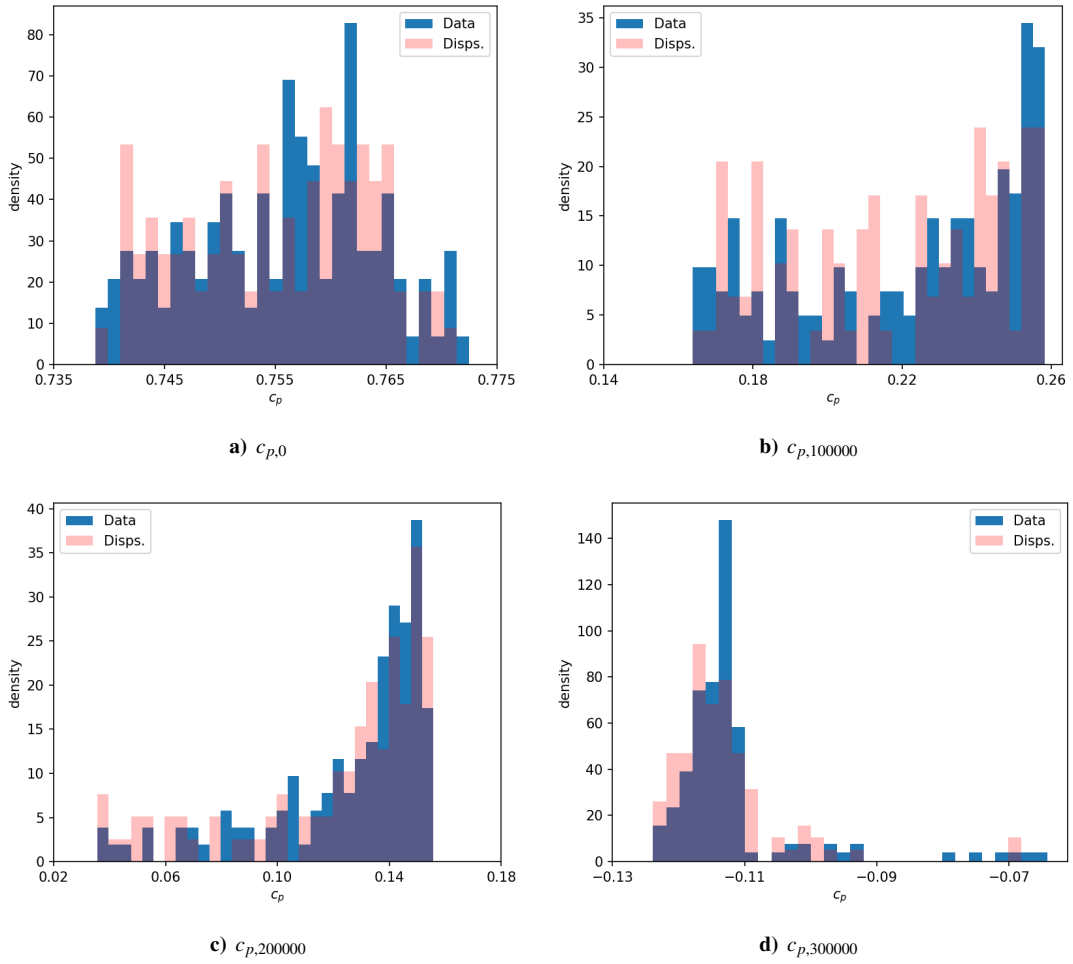


Figure 3. MVN-Copula c_p histograms for 100 integrated aerodynamic coefficient sets taken from known dataset.

Coefficient	Critical Value	Score
c_p	0.0260077	0.0192575

Table 1. MMD 2-sample test results on MVN-Copula generated surface pressures' Ω coefficients.

B. Leave-One-Out Error Estimation

Once the method passed the previous validation test, the error in the generated surface pressures was approximated using leave-one-out (LOO) error estimation. In order to estimate this, each of the n_c=29 CFD cases was removed from the dataset one at a time and then the method was used to predict the left out surface pressure. The mean error at each surface pressure point was then taken to be the leave-one-out error approximation of the method.

Figure 4 shows the leave-one-out error estimation for each of the 402909 surface pressure points. The red data is the maximum absolute value seen amongst the n_c known cases, the black data is the error estimate. The dimensionality of the data makes a complete visualization of these results difficult. Figure 5 shows a histogram plot of the ratio of the leave-one-out error to the max absolute value of the c_p at each index. The average value of this ratio is 0.059 while the maximum value is 0.71. This shows that the predictive performance of the method on average is decent, however there are surface pressure points where it struggles to make accurate predictions. The scale of the error estimate seems reasonable on average but there is always a chance that the leave-one-out error will dominate at surface pressure locations with small absolute magnitudes, which appears to be happening at the index with the maximum ratio value. In order to get a better idea of the acceptability of the scale of these errors, the leave-one-out error will be applied to surface pressures that have accounted for a simulated aleatoric uncertainty in the next results section. This will exhibit a comparison of the relative magnitudes of the realized aleatoric uncertainty to the leave-one-out error, which is more indicative of the method's overall performance.

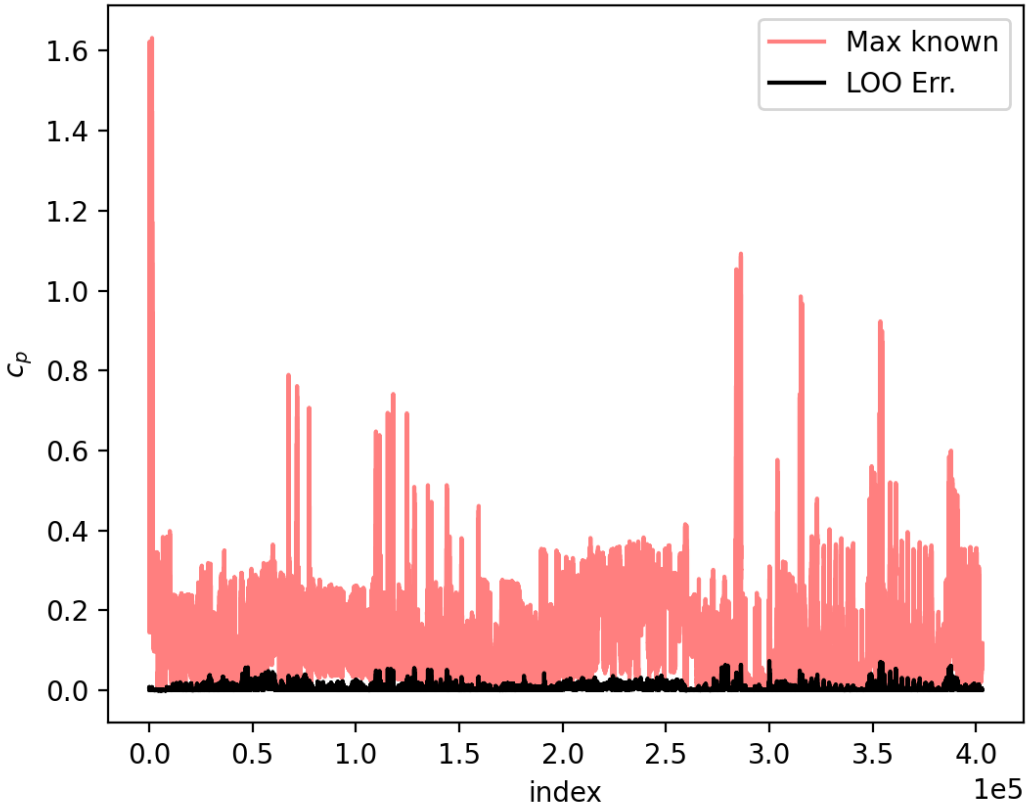


Figure 4. Leave-one-out errors for 29 known data points, 20k copula draws

C. Simulated Uncertainty

A simulated aleatoric uncertainty is applied to the integrated coefficients and surface pressures are generated using the copula-based methods. The aleatoric uncertainties were simulated according to $\tilde{C}^i_{z,j} = C^i_z(1 + \epsilon_{U,j})$, where C^i_z is the integrated coefficient z from the $i-$th known data case and $\epsilon_{U,j}$ is a value drawn from the aleatoric uncertainty model. The same $\epsilon_{U,j}$ was used for related forces and moments, for example one $\epsilon_{U,j}$ was drawn for normal force and then used to generate $\tilde{C}^i_{N,j}$ and $\tilde{C}^i_{LM,j}$. The $\epsilon_{U,j}$ are drawn from two different distributions to model the uncertainty, $\epsilon_U = \mathcal{N}(0, 0.0333)$ and $\epsilon_U = \mathcal{U}(-0.1, 0.1)$. This is done to compare the difference in using two commonly assumed aleatoric uncertainty models. The justification of the somewhat arbitrarily chosen bounds of these uncertainty distributions is discussed at the end of this section. The leave-one-out error estimates from the previous sections are added to these generated surface pressures and a probability box is created for each surface pressure point. The probability box is presented to be a more complete description of the total uncertainty at each surface pressure data point, accounting for both model error and simulated aleatoric uncertainty sources.

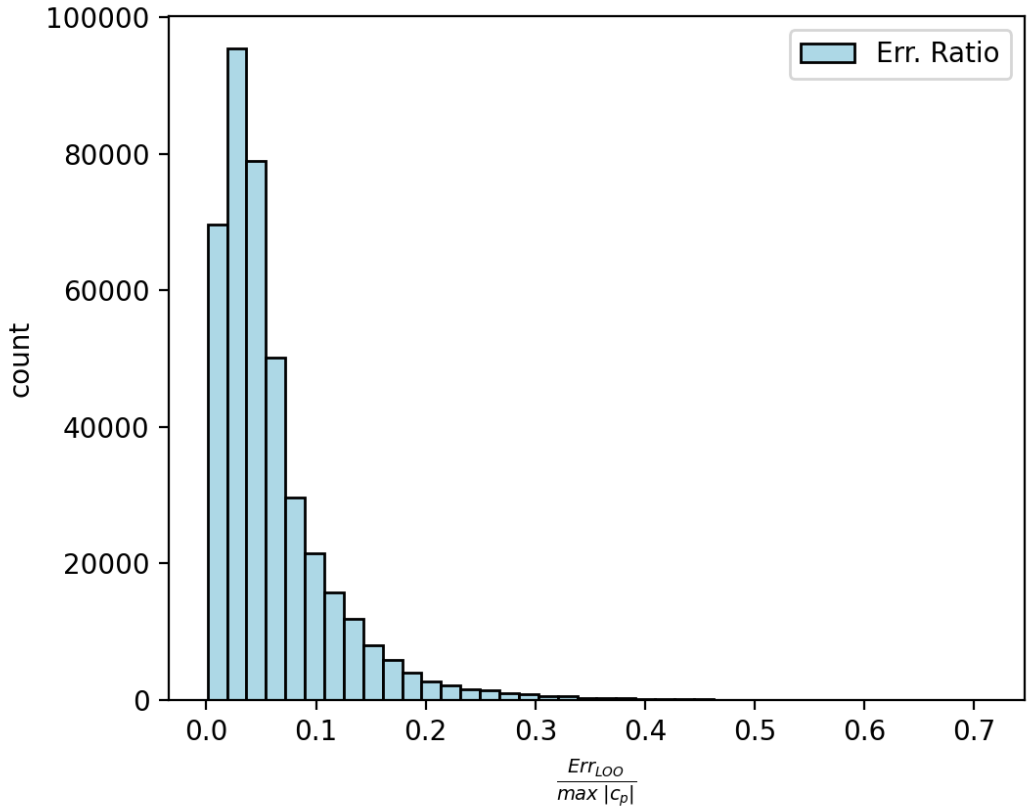


Figure 5. Ratio of leave-one-out errors to max absolute c_p for 29 known data points, 20k copula draws

It is not possible to show even a small fraction of the over 400000 probability boxes generated from this data, but several are included in Figures 6 - 8. Figure 6 shows the probability boxes for four different surface pressure points along the vehicle. The black line used the normal distribution uncertainty model, and the blue line used the uniform distribution. The data labeled $c_{p,0}$ is the probability box at the first surface pressure data point, $c_{p,1}$ would be the probability box at the second surface pressure data point and so on. The figures show how the copula method allows for spatial dependence in the uncertain surface pressure realizations of the aleatoric uncertainty in the integrated coefficients. For some surface pressure points, like those as the one shown in Figure 6b, the leave-one-out error is approximately the same magnitude as the aleatoric uncertainty and both have similar contributions to the width of the probability box. However, in the case of Figure 6a, the aleatoric uncertainty is larger and contributes more to the overall uncertainty of that surface pressure point. The different aleatoric uncertainty models do show some differences in the resulting probability boxes depending on the surface pressure locations. For the included figures, there is not too much difference between the shapes of the probability boxes, depending just on the aleatoric uncertainty model. This is to be expected since the draws from the different aleatoric uncertainties are realized in the method as two different sets of integrated coefficients that have similar minimum and maximum bounds. The normal distribution could draw values far outside the uniform distribution bounds, however, by design, the 3-sigma bounds are similar.

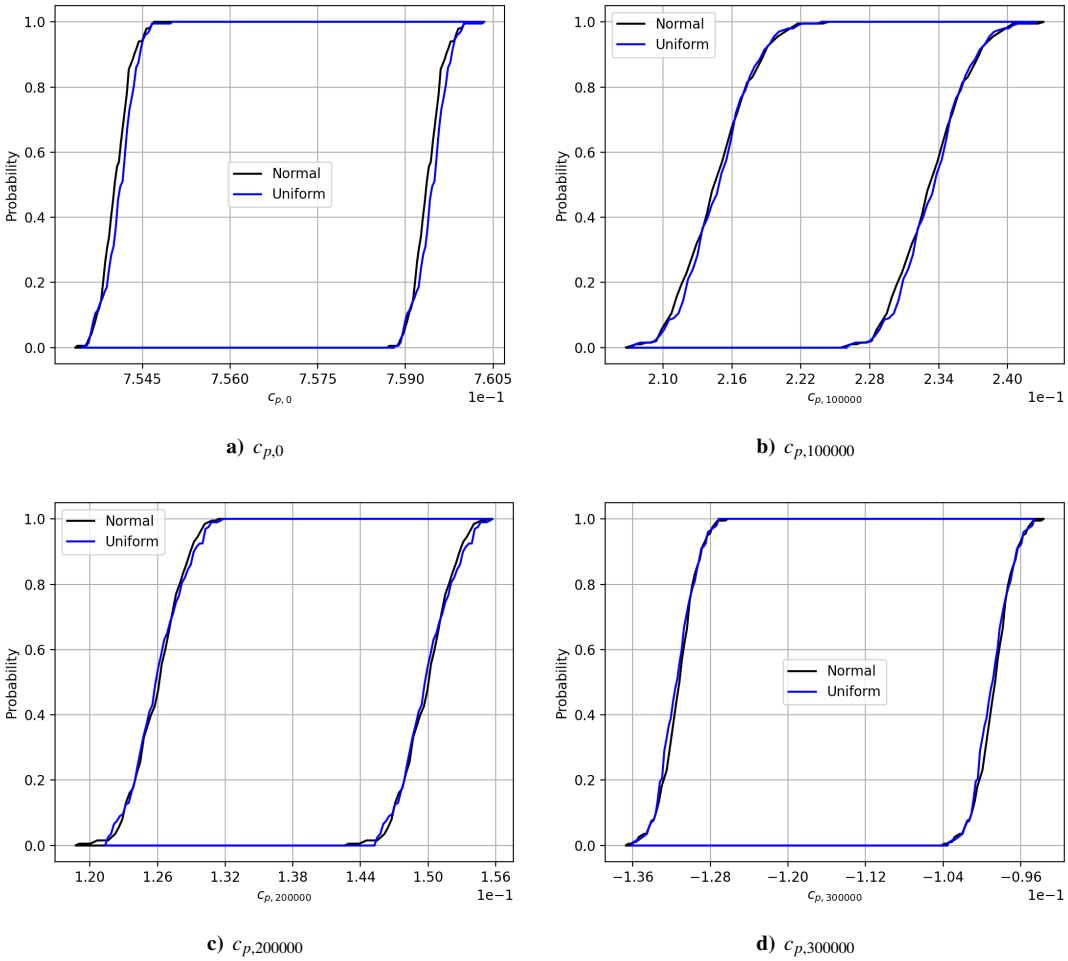
Figure 7 shows the probability boxes for the four surface pressure points that had the largest values for the ratio shown in Figure 5. The probability boxes for these points don't show significantly wider boxes as might be expected due to having the largest relative errors. Although the largest seen difference between normal and uniform uncertainty occurs in Figure 7b. Figures 8 shows the probability boxes for the four surface points that had the largest leave-one-out error ratio values shown in Figure 4. This figure shows that it doesn't appear that a large leave-one-out error ratio necessarily corresponds to a wider probability box. The overall proportions of these probability boxes are impacted by the balance between the leave-one-out error and the aleatoric uncertainty.

The differences between the aleatoric models is not expected, it is suspected to be due to natural probability variances of sampling with a low number of random samples. To investigate this, the number of drawn uncertain integrated samples was doubled to 400 and the probability boxes from those results are shown in Figure 9. Two probability boxes from Figures 7 and 8 were chosen for comparison in this figure, and it appears that the difference between the two aleatoric model's probability boxes becomes smaller with a larger number of random samples. However, there is a still a difference between the two aleatoric models that is driven by the uniform model being much more likely to draw values near the bounds of its distribution. This would change with a huge number of samples however, where now the normal distribution could likely sample a value beyond its three sigma bounds thus beyond the used uniform distribution's bounds. The key observation is that the aleatoric model doesn't have an impact on the shapes of the probability bounds as the number of randomly drawn integrated values increases. Therefore, with large enough sampling, the difference between the probability boxes using different aleatoric models is seen as a result of the possible minimum and maximum values.

While the probability boxes look reasonable, this is more of a comparison of the difference in relative magnitude between the leave-one-out error estimate and the, arbitrarily, chosen aleatoric model. The probability boxes would look much differently if, for example, $\mathcal{U}(-0.01, 0.01)$ was used in place of $\mathcal{U}(-0.1, 0.1)$. In this new case, the leave-one-out error would be unchanged and would now dwarf the aleatoric uncertainty, thus the probability boxes would look much wider and square-like. This leads to the question of is the chosen aleatoric uncertainty models realistic for a real-world database scenario? While it is difficult to find published numbers on launch vehicle uncertainties, the work in [13] provides a comparison of axial force coefficient results across different CFD solvers, reporting percent differences of around 10 to 20 percent across various mach numbers. The aleatoric uncertainty used in the simulated uncertainty results in this chapter represents approximately a 10 percent uncertainty in each integrated coefficient. Thus, it seems like a relatively conservative test of uncertainty considering that this type of solver-to-solver comparison term is often included in a total uncertainty term used in aerodynamic databases. For example, [14] reports a CART3D-to-OVERFLOW comparison term in the authors' total uncertainty build up, where this term is never the largest contributor for any aerodynamic coefficient. This gives confidence that the simulated uncertainty presented here is a conservative test of the method's performance in a practical scenario where the complete uncertainty quantification term would be much larger.

Conclusion

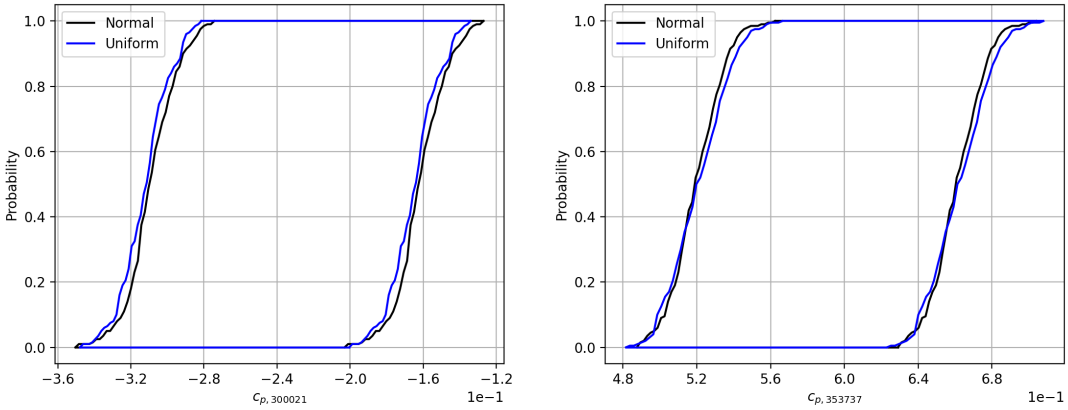
The goal for this work was to provide a method that can generate statistically consistent surface pressures according to uncertain integrated forces and moments. The uncertainty of the force and moment database was used as it typically includes higher fidelity data that will result in a higher quality quantified uncertainty. The results are promising as the copula-based method was able to pass the Maximum Mean Discrepancy two-sample test that was chosen for validation. The method is shown to perform well in the conservative simulated uncertainty scenario while accounting



a) $c_{p,0}$ **b)** $c_{p,100000}$

c) $c_{p,200000}$ **d)** $c_{p,300000}$

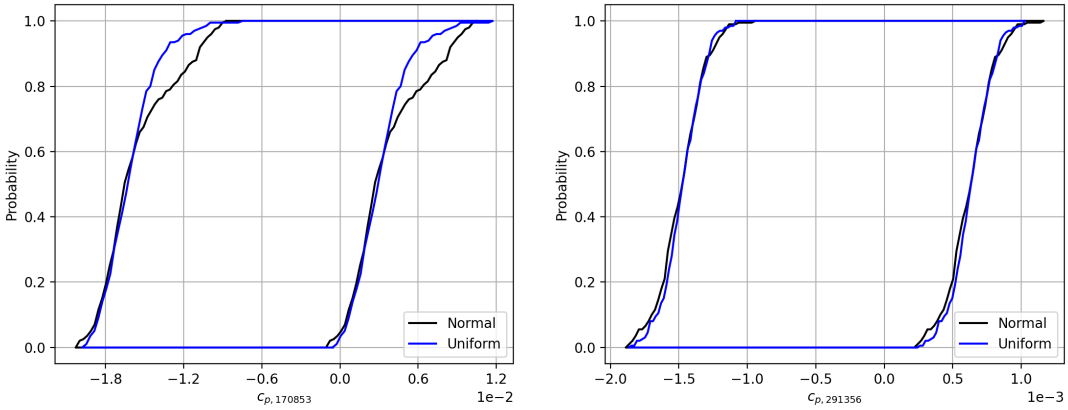
Figure 6. MVN-Copula c_p probability boxes for simulated uncertainty.



a) $c_{p,300021}$ **b)** $c_{p,353737}$

c) $c_{p,353736}$ **d)** $c_{p,353765}$

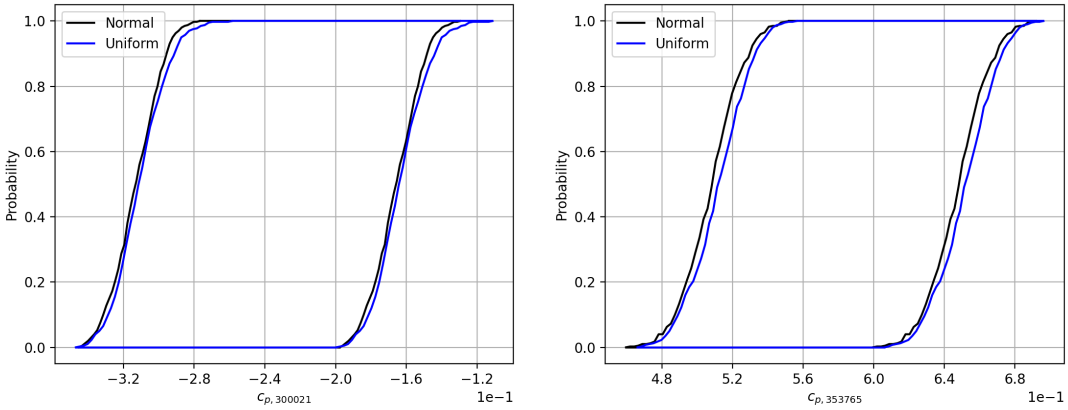
Figure 7. MVN-Copula c_p probability boxes for simulated uncertainty for locations of largest leave-one-out error.



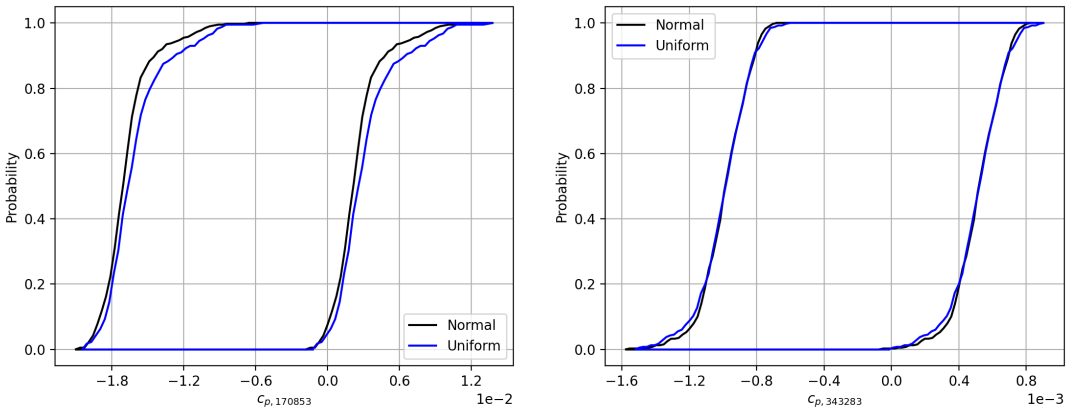
a) $c_{p,170853}$ **b)** $c_{p,291356}$

c) $c_{p,291355}$ **d)** $c_{p,343283}$

Figure 8. MVN-Copula c_p probability boxes for simulated uncertainty for locations of largest leave-one-out error ratios.



a) $c_{p,300021}$ **b)** $c_{p,353737}$



c) $c_{p,170853}$ **d)** $c_{p,343283}$

Figure 9. MVN-Copula c_p dense probability boxes for simulated uncertainty for select locations.

for the estimated leave-one-out error. Overall, the copula-based method was relatively successful as an approach that can generate statistically consistent surface pressures according to uncertain integrated values. The described method allows for the construction of a surface pressure database with uncertainty which opens up many potential analysis pathways. For example, an interesting use case for these uncertain surface pressures could be to provide the sensitivity of surface pressures at critical points on the vehicle to database variables such as angle of attack or angle of sideslip.

A potential avenue for future work is to explore capability of the copula-based method to provide any number of surface pressures for a given set of integrated coefficient values, including a corresponding estimate for the probability density of each generated distributed load. This allows for the ability to differentiate the generated loads by the estmated probability density or select the surface pressures which the model outputs as being more likely. Another potential area of research is exploring different approaches to approximating the high-dimensional statistical distribution required by the described copula-based method. An example would be to use a Bayesian Sequential Partitioning [15] approach in order to generate a high-dimensional histogram that would approximate the required distribution. An initial investigation of using this method provided inferior results to those shown in this work, however the results were promising enough that additional development time could be justified.

Acknowledgments

Resources supporting this work were provided by the NASA High-End Computing Capability (HECC) program through the NASA Advanced Supercomputing (NAS) Division at Ames Research Center. This work was funded by the Space Launch System (SLS) Program in the Exploration Systems Development Misson Directorate (ESDMD). The authors also thank Stuart E. Rogers, Jamie G. Meeroff, Daniel G. Schauerhamer, and Joshua F. Diaz from the Ames SLS CFD team for discussions and support.

References

[1] Shea, P. R., Pinier, J. T., Houlden, H., Favaregh, A., Hemsch, M. J., Dalle, D. J., Rogers, S. E., Meeroff, J., and Lee, H. C., "Ascent Aerodynamic Force and Moment Database Development for the Space Launch System," *AIAA Aviation 2019 Forum*, 2019.

[2] McMillin, S. N., Shea, P. R., Dalle, D. J., Rogers, S. E., Roozeboom, N., Meeroff, J., and Lee, H. C., "Comparison of Space Launch System Aerodynamic Surface Pressure Measurements from Experimental Testing and CFD," *AIAA Aviation 2019 Forum*, 2019.

[3] Dalle, D. J., Rogers, S. E., Burkhead, A. C., and Meeroff, J., "Distribution of SLS Integrated Load Uncertainty to Surface Pressures and Sectional Loads," *ICCFD11 Conference 2022*, 2022.

[4] Gretton, A., Borgwardt, K. M., Rasch, M. J., Schölkopf, B., and Smola, A., "A Kernel Two-Sample Test," *Journal of Machine Learning Research*, Vol. 13, No. null, mar 2012, pp. 723–773.

[5] Murman, S. M. and Diosady, L. T., "Simulation of a Hammerhead Payload Fairing in the Transonic Regime," *54th AIAA Aerospace Sciences Meeting*, 2016, AIAA Paper 2016-1548.

[6] Barth, T., "An Overview of Combined Uncertainty and A-Posteriori Error Bound Estimates for CFD Calculations," *54th AIAA Aerospace Sciences Meeting*, 2016, AIAA Paper 2016-1062.

[7] Biedron, R. T., Calrson, J., Derlaga, J. M., Gnoffo, P. A., Hammond, D. P., Jacobson, K. E., Jones, W. T., Kleb, B., Lee-Rausch, E. M., Nielson, E. J., Park, M. A., Rumsey, C. L., Thomas, J. L., Thompson, K. B., Walden, A. C., Wang, L., and Wood, W. A., "FUN3D Manual: 13.7," Tech. Rep. TM-20205010139, NASA, 2020.

[8] Dalle, D. J., Rogers, S. E., Lee, H. C., and Meeroff, J., "Adjustments and Uncertainty Quantification for SLS Aerodynamic Sectional Loads," *2018 Applied Aerodynamics Conference*, 2018.

[9] Burkhead, A. C. and Dalle, D. J., "Statistically Consistent Dispersion of Line Loads to Uncertain Integrated Forces and Moments," *AIAA SCITECH 2024 Forum*, 2024.

[10] Nelsen, R., *An Introduction to Copulas*, Springer, New York, NY, USA, 1999.

[11] Scott, D. W. and Sain, S. R., "Multidimensional Density Estimation," *Data Mining and Data Visualization*, edited by C. Rao, E. Wegman, and J. Solka, Vol. 24 of *Handbook of Statistics*, Elsevier, 2005, pp. 229–261.

[12] Wang, Z. and Scott, D. W., "Nonparametric density estimation for high-dimensional data—Algorithms and applications," *WIREs Computational Statistics*, Vol. 11, No. 4, 2019, pp. e1461.

[13] Kiris, C., Housman, J., Gusman, M., Schauerhamer, D., Deere, K., Elmiligui, A., Abdol-Hamid, K., Parlette, E., Andrews, M., and Blevins, J., "Best Practices for Aero-Database CFD Simulations of Ares V Ascent," *49th AIAA Aerospace Sciences Meeting including the New Horizons Forum and Aerospace Exposition*, 2011.

[14] Chan, D. T., Dalle, D. J., Rogers, S. E., Pinier, J. T., Wilcox, F. J., and Gomez, R. J., "Space Launch System Booster Separation Aerodynamic Database Development and Uncertainty Quantification," *54th AIAA Aerospace Sciences Meeting*, 2016.

[15] Luo Lu, H. J. and Wong, W. H., "Multivariate Density Estimation by Bayesian Sequential Partitioning," *Journal of the American Statistical Association*, Vol. 108, No. 504, 2013, pp. 1402–1410.